

Continuous Variables (2,3) Threshold Quantum Secret Sharing Schemes

Andrew M. Lance,¹ Thomas Symul,¹ Warwick P. Bowen,¹ Tomáš Tyc,^{2,3} Barry C. Sanders,² and Ping Koy Lam¹

¹*Quantum Optics Group, Department of Physics, Faculty of Science, Australian National University, ACT 0200, Australia*

²*Department of Physics and the Centre for Advanced Computing - Algorithms and Cryptography, Macquarie University, Sydney, NSW 2109, Australia*

³*Institute of Theoretical Physics, Masaryk University, 61137 Brno, Czech Republic*

(Dated: October 26, 2018)

We present two experimental schemes to perform continuous variable (2,3) threshold quantum secret sharing on the quadratures amplitudes of bright light beams. Both schemes require a pair of entangled light beams. The first scheme utilizes two phase sensitive optical amplifiers, whilst the second uses an electro-optic feedforward loop for the reconstruction of the secret. We examine the efficacy of quantum secret sharing in terms of fidelity, as well as the signal transfer coefficients and the conditional variances of the reconstructed output state. We show that both schemes in the ideal case yield perfect secret reconstruction.

PACS numbers: 03.67.Dd, 42.50.Dv, 42.50.Lv, 42.65.Yj

I. INTRODUCTION

Quantum secret sharing (QSS) has attracted a lot of attention recently as an important primitive for protecting quantum information. QSS, originally proposed as a means to protect classical information using laws of quantum physics [1], has developed into a general theory describing a secure transmission of quantum information to a group of parties (players), not all of whom can be trusted. The collaboration of the players is essential in order to recover the quantum information. This general approach to QSS is the quantum analogue of classical secret sharing [2].

A QSS protocol involves a dealer who holds a secret state (quantum information) $|\psi_{\text{in}}\rangle$, encodes it into an entangled state $|\Psi\rangle$ over n quantum sub-systems (shares) and distributes the shares to n players. The encoding is done in such a way that only specified subsets of the players (the access structure) are able to extract the secret while all other subsets (forming the adversary structure) are unable to learn anything about it. The reconstruction of the secret by the collaborating players is then achieved by applying a suitable joint unitary operation on their shares, which disentangles one share from all the others and yields the secret state.

Among QSS protocols, there is an important class of so-called (k, n) threshold schemes [3], in which the access structure consists of all groups of k or more players while there are n players in total. This makes the protocol “fair” in the sense that no player is favored among others. The simplest threshold scheme is the $(2, 2)$ scheme where there are only two players and both have to collaborate to retrieve the secret. The implementation of this scheme is, in general, very simple. The dealer only needs to interfere the quantum secret on a beam splitter with a noisy beam, each player receiving one of the outputs. It is impossible to obtain any information about the secret state through operations on either share independently due to the contamination of the noisy beam. The secret can be perfectly reconstructed, however, if the players co-operate by interfering their shares on another 1:1 beam splitter.

A continuous variable (2,3) QSS threshold schemes has been proposed by Tyc and Sanders [4]. This scheme uses

electromagnetic field modes, and employs interferometers for both the encoding and decoding of the secret. In this paper, we extend the original proposal by Tyc and Sanders and introduce another more practical scheme that utilizes an electro-optic feedforward technique. We consider the secret to be encoded on the sideband frequency quadrature amplitudes of a light beam. Ideally the dealer would employ a perfectly entangled pair of beams. This is in practice impossible, however, improvement over classical schemes can still be achieved with finite amounts of entanglement. Moreover we will show that the introduction of classical noise by the dealer can further improve the QSS scheme. We compare and quantify the performances of both schemes in terms of available input entanglement using two measures. We use the fidelity between input and output states as a figure of merit. We also characterize QSS in terms of the signal transfer coefficients and the conditional variances of both conjugate quadrature amplitudes of the secret.

The paper is organized in the following manner. In Section II we present the dealer protocol to generate three shares. We outline, in Section III, the central role of the optical parametric processes in the QSS schemes. We then present the two secret sharing schemes in Section IV and characterize these schemes in Section V.

II. (2,3) THRESHOLD SCHEME

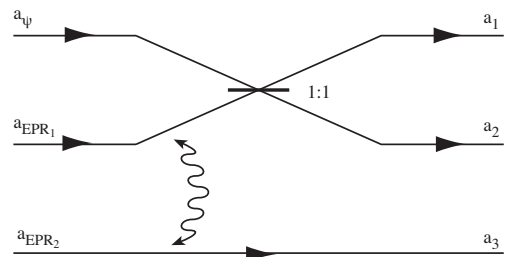


FIG. 1: Dealer protocol for the production of three shares in a (2,3) threshold QSS scheme.

Figure 1 shows the dealer protocol of a (2,3) threshold QSS scheme as proposed by Tyc and Sanders [4]. The dealer employs a pair of entangled beams to encode the secret by interfering one of them with the secret state on a 1:1 beam splitter. We let \hat{a}_ψ , \hat{a}_{EPR1} and \hat{a}_{EPR2} denote the annihilation operators corresponding to the secret and the two entangled beams, respectively. The linearized expression for the annihilation operator is given by $\hat{a}(t) = \alpha + \delta\hat{a}(t)$ where α and $\delta\hat{a}(t)$ denote the steady state component and zero mean value fluctuations of the annihilation operator, respectively. The amplitude and phase quadrature operators are denoted as $\hat{X}^+ = \hat{a}^\dagger + \hat{a}$ and $\hat{X}^- = i(\hat{a}^\dagger - \hat{a})$, whilst the variance of these operators is expressed in the frequency domain as $V^\pm(\omega) = \langle [\delta\hat{X}^\pm(\omega)]^2 \rangle$. The annihilation operators corresponding to the three shares are then given by

$$\hat{a}_1 = \frac{\hat{a}_\psi + \hat{a}_{\text{EPR1}}}{\sqrt{2}} \quad (1)$$

$$\hat{a}_2 = \frac{\hat{a}_\psi - \hat{a}_{\text{EPR1}}}{\sqrt{2}} \quad (2)$$

$$\hat{a}_3 = \hat{a}_{\text{EPR2}} \quad (3)$$

Similar to the (2,2) secret sharing scheme discussed earlier, players 1 and 2 (henceforth denoted by $\{1,2\}$) only need to complete a Mach-Zehnder interferometer with the use of a 1:1 beam splitter to retrieve the secret state. The output beams of the Mach-Zehnder are described by

$$\hat{a}'_1 = \frac{\hat{a}_1 + \hat{a}_2}{\sqrt{2}} = \hat{a}_\psi \quad (4)$$

$$\hat{a}'_2 = \frac{\hat{a}_1 - \hat{a}_2}{\sqrt{2}} = \hat{a}_{\text{EPR1}} \quad (5)$$

Eq. (4) clearly shows that the secret is perfectly reconstructed. In contrast, secret reconstructions for $\{2,3\}$ or $\{1,3\}$ require more complex protocols. The paper now focuses on experimental alternatives for the implementation of this reconstruction process.

III. OPTICAL PARAMETRIC GAIN AND ENTANGLEMENT

One of the important element for QSS is the optical parametric down conversion process. In this process a pump photon is converted into a pair of twin photons following the simple scheme: $\hbar\omega_{\text{pump}} \rightarrow \hbar\omega_s + \hbar\omega_i$, where the signal and idler modes are denoted ω_s and ω_i , respectively.

A. Type II system

This down conversion can be achieved in a bulk Type II second order non-linear crystal in a traveling wave configuration. By treating the pump as a classical beam, we find the input-output relations for the signal and idler annihilation operators to be [6]

$$\hat{a}_{s,\text{out}} = \hat{a}_{s,\text{in}} \cosh r + \hat{a}_{i,\text{in}}^\dagger \sinh r \quad (6)$$

$$\hat{a}_{i,\text{out}} = \hat{a}_{i,\text{in}} \cosh r + \hat{a}_{s,\text{in}}^\dagger \sinh r \quad (7)$$

where \hat{a}_s and \hat{a}_i are the annihilation operators of the signal and the idler modes, respectively. The interaction parameter is $r = \gamma t$, where γ is proportional to the pump field amplitude and the second order susceptibility coefficient of the crystal. By choosing \hat{a}_p and \hat{a}_q to be the $\pm 45^\circ$ polarized modes defined by $\hat{a}_{p,q} = (\hat{a}_s \pm \hat{a}_i)/\sqrt{2}$ and assuming that all the power is carried by mode \hat{a}_p , Eq. (6) and Eq. (7) give

$$\hat{a}_{p,\text{out}} = \hat{a}_{p,\text{in}} \cosh r + \hat{a}_{p,\text{in}}^\dagger \sinh r \quad (8)$$

from which we can deduce the total number of photons at the output $\langle \hat{N}_{p,\text{out}} \rangle = G(\phi)N_o$ with gain

$$G(\phi) = \cosh 2r + \sinh 2r \cos \phi \quad (9)$$

where $\phi = \phi_{\text{pump}} - 2\phi_p$ is the phase mismatch between the pump and the \hat{a}_p mode. The gain $G(\phi)$ oscillates between the two values $G_0 = e^{2r}$ and e^{-2r} , depending of the relative phase between the input and the pump beam. Finally we note that the output quadrature amplitudes are given by

$$\hat{X}_{p,\text{out}}^+ = \sqrt{G_0} \hat{X}_{p,\text{in}}^+ \quad (10)$$

$$\hat{X}_{p,\text{out}}^- = \frac{1}{\sqrt{G_0}} \hat{X}_{p,\text{in}}^- \quad (11)$$

B. Type I system

Another way of performing the optical parametric down conversion process is by using a Type I crystal. Optical parametric oscillators (OPO) operating below threshold can exhibit phase sensitive amplification [7]. We assume the OPO is a simple Fabry-Perot cavity with a second order non-linear gain medium. The equations of motion for a general OPO cavity are given by

$$\dot{a} = \gamma\hat{a} - \kappa\hat{a} + \sqrt{2\kappa_b}\hat{A}_b + \sqrt{2\kappa_f}\hat{A}_f + \sqrt{2\kappa_l}\delta\hat{A}_l \quad (12)$$

$$\dot{a}^\dagger = \gamma^*\hat{a}^\dagger - \kappa\hat{a}^\dagger + \sqrt{2\kappa_b}\hat{A}_b^\dagger + \sqrt{2\kappa_f}\hat{A}_f^\dagger + \sqrt{2\kappa_l}\delta\hat{A}_l^\dagger \quad (13)$$

where \hat{A}_f and \hat{A}_b are the inputs into the front and back mirrors and $\delta\hat{A}_l$ is a vacuum fluctuation term due to loss in the cavity. $\kappa = \kappa_f + \kappa_b + \kappa_l$ is the total cavity damping rate, where κ_f , κ_b and κ_l are the damping rates of the front and back mirrors and the loss in the cavity respectively.

The output from the OPA expressed in terms of an input \hat{A}_f can be derived from Eq. (12) and Eq. (13). By setting $\kappa_b = 0$ and $\kappa_l = 0$, so that no vacuum fluctuation couple into the cavity, the output field quadratures from the OPA expressed in the frequency domain are

$$X_{\text{out}}^+(\omega) = \frac{\kappa_f - i\omega + \gamma}{i\omega + \kappa - \gamma} X_f^+(\omega) \quad (14)$$

$$X_{\text{out}}^-(\omega) = \frac{\kappa_f - i\omega - \gamma}{i\omega + \kappa + \gamma} X_f^-(\omega) \quad (15)$$

where the general operator $Z = Z(\omega)$ is the Fourier transform of the time operator $\hat{Z} = \hat{Z}(t)$. By assuming the frequency is

small such that $\omega \ll \kappa_f$, the output field quadratures can be expressed more succinctly as

$$X_{\text{out}}^+ = \sqrt{G} X_f^+ \quad (16)$$

$$X_{\text{out}}^- = \frac{1}{\sqrt{G}} X_f^- \quad (17)$$

where the gain is defined as $\sqrt{G} = (\kappa_f + \gamma)/(\kappa_f - \gamma)$. The amount of gain is dependent on the pump power, and on the relative phase between the pump and input beams. In the amplification regime phase squeezed light is produced, whilst in the deamplification regime amplitude squeezed light is produced.

C. Production of entangled beams

For Type II systems, the signal and idler output modes generated by a single PSA, as defined in Eq. (6) and (7), exhibit quadrature entanglement [8, 9]. Since the two modes are orthogonally polarized, the entangled beams can be spatially separated using a polarizing beam splitter. Whilst for Type I systems, quadrature entangled beams can be produced by interfering a pair of squeezed beams produced by two OPAs on a 1:1 beam splitter [10]. The output beams from the beam splitter also will exhibit quadrature entanglement.

The entanglement between the X^+ and X^- quadratures of the output modes in both systems can be characterized by using the inseparability criterion proposed by Duan *et al.* [11]. For symmetric inputs, Duan's inseparability criterion is given by

$$\langle (\delta X_s^+ + \delta X_i^+)^2 \rangle + \langle (\delta X_s^- - \delta X_i^-)^2 \rangle < 2 \quad (18)$$

where subscripts s and i denote the two entangled beams. Since $\langle (\delta X_s^+ + \delta X_i^+)^2 \rangle = \langle (\delta X_s^- - \delta X_i^-)^2 \rangle = 1/\cosh 2r$ for both configurations, the beams show quadrature entanglement when $r > 0$ (Where r is the squeezing parameter of the input beams for Type I, or the interaction parameter for Type II).

IV. PROPOSED EXPERIMENTAL SETUPS

In this section, we analyze how $\{2,3\}$ can reconstruct the secret sent by the dealer. The method described here can also be applied unchanged to $\{1,3\}$, and so we will not cite explicitly this case in the following paragraphs.

First, one can remark that by performing homodyne measurement on \hat{a}_2 and \hat{a}_3 , and then by combining their results

with a well chosen gain, $\{2,3\}$ can get a measure of the amplitude or the phase of the secret, but they can not measure both at the same time. This scheme can be used for practical applications which require only classical information of a single quadrature to be transferred between the dealer and the players. Since the secret is not reconstructed, nor quantum information of both quadratures transferred, this protocol does not qualify as QSS.

Let us now concentrate on schemes which effectively reconstruct both the amplitude and phase of the secret at the same time.

A. The 2PSA scheme

This scheme follows the original idea of Tyc and Sanders [4]. To reconstruct the secret using two PSAs, $\{2,3\}$ first combine \hat{a}_2 and \hat{a}_3 on a 1:1 beam splitter, producing two beams \hat{a} and \hat{b} , as depicted in Fig. 2. They pass each of these beams through separate PSAs, denoted by PSA_a and PSA_b respectively. Both the PSAs are adjusted so that the output of PSA_a is amplified in the X^+ quadrature and deamplified in the X^- quadrature whilst the PSA_b output is deamplified in the X^+ quadrature and amplified in the X^- quadrature. The gain of both PSAs is assumed to be equal. The final step required for reconstruction of the secret is to combine both PSA outputs on another 1:1 beam splitter. We denote these outputs as $\hat{a}_{\text{out}1}$ and $\hat{a}_{\text{out}2}$.

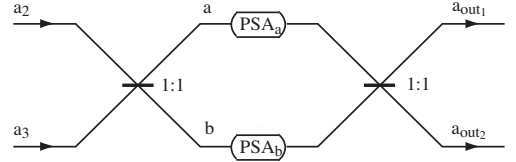


FIG. 2: Reconstruction of secret for $\{2,3\}$ using the 2PSA scheme.

The PSAs can be used in both configurations discussed in Section III. We find the output quadrature amplitudes for both configurations to be of the form

$$X_{\text{out}1}^\pm = \frac{1}{2\sqrt{2}} X_\psi^\pm \left(\sqrt{G} + \frac{1}{\sqrt{G}} \right) + \frac{\alpha^\pm}{\sqrt{2}} + \frac{\beta^\pm}{\sqrt{2}} \quad (19)$$

It is obvious that if output 1 is used to construct the secret, then output 2 will in the limit of perfect QSS contain no relevant information. We will therefore not analyse output 2. For the Type II configuration, the α^\pm and β^\pm parameters are dependent on the interaction parameters of the parametric process

$$\alpha^\pm = \left[\sqrt{G} \left(\frac{1}{\sqrt{2}} \sinh r - \frac{1}{2} \cosh r \right) - \frac{1}{\sqrt{G}} \left(\frac{1}{2} \cosh r + \frac{1}{\sqrt{2}} \sinh r \right) \right] X_{s,\text{in}}^\pm \quad (20)$$

$$\beta^\pm = \left[\sqrt{G} \left(\frac{1}{\sqrt{2}} \cosh r - \frac{1}{2} \sinh r \right) - \frac{1}{\sqrt{G}} \left(\frac{1}{2} \sinh r + \frac{1}{\sqrt{2}} \cosh r \right) \right] X_{i,\text{in}}^\pm \quad (21)$$

For the Type I configuration, they are dependent on the amount of squeezing of both squeezed state inputs. We therefore obtain

$$\alpha^\pm = \frac{X_{\text{sqz}1}^\mp}{\sqrt{G}}(-1 \mp \sqrt{2}) + \sqrt{G}(-1 \pm \sqrt{2}) \quad (22)$$

$$\beta^\pm = \frac{X_{\text{sqz}2}^\pm}{\sqrt{G}}(-1 \pm \sqrt{2}) + \sqrt{G}(-1 \mp \sqrt{2}) \quad (23)$$

In the case of perfect entanglement (i.e. $r \rightarrow \infty$), setting the parametric gain to

$$G = \frac{\sqrt{2} + 1}{\sqrt{2} - 1} \quad (24)$$

will completely eliminate the contribution of the input entanglement modes. We are therefore left with the original secret. With imperfect entanglement, we find for the Type II configuration

$$X_{\text{out}1}^\pm = X_\psi^\pm - e^{-r} X_{s,\text{in}}^\pm + e^{-r} X_{i,\text{in}}^\pm \quad (25)$$

Similarly, the output quadrature amplitudes for the Type I configuration are given by

$$X_{\text{out}1}^+ = X_\psi^+ - \sqrt{2} X_{\text{sqz}2}^+ \quad (26)$$

$$X_{\text{out}1}^- = X_\psi^- - \sqrt{2} X_{\text{sqz}1}^+ \quad (27)$$

where it is assumed that $X_{\text{sqz}1,2}^\pm$ are the squeezed quadratures. The results above demonstrate that with finite entanglement, $\{2,3\}$ are able to reconstruct the secret \hat{a}_ψ with added noise variance of $2e^{-2r}$. In addition to the parametric processes required for the generation of a pair of entangled beams, the QSS scheme described above requires two additional PSAs. This is experimentally very challenging. Since non-linear effects in optics are small, there have been methods used to increase optical intensities in experiments to enhance the parametric process. One such example is the utilization of high peak power pulsed light sources, either in Q-switched or mode-locked setups, to single pass light beams through the non-linear mediums to achieve the required phase sensitive amplification. A common difficulty found in such systems is the distortion of optical wave fronts due to the non-linear medium. This would result in poor optical interference and losses. Another method of increasing optical intensity in non-linear processes is the use of optical resonators. In this situation, the resonators also act as mode cleaners to the beams, thus ensuring better beam quality. However, impedance matching of the resonators, which is not required for single-pass phase sensitive amplification, is difficult to achieve. Imperfect impedance matching again leads to losses. It is therefore interesting to find an alternative scheme which does not require additional parametric processes for the reconstruction of the secret. In the next section, we will present a QSS scheme that requires only an electro-optic feedforward loop for $\{2,3\}$ in secret reconstruction.

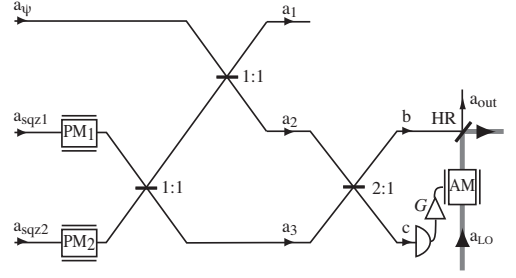


FIG. 3: Dealer protocol and the reconstruction of secret for $\{2,3\}$ using an electro-optic feedforward loop. 2:1 is a 2/3 reflective beam splitter and HR is a highly reflective beam splitter. PM_{1,2} are phase modulators on the respective amplitude squeezed beams.

B. Feedforward loop scheme

Electro-optic feedforward loops have been widely used in many continuous variable experiments. The feedforward setup has been demonstrated to be useful in noiseless control of light beams [12] and has recently been used in teleportation experiments [14, 15]. In our feedforward QSS scheme, the dealer is required to add classical noise on the entangled beams. The purpose of adding classical noise will be discussed in the characterization Section V. This can be achieved using a pair of phase modulators on the constituent amplitude squeezed beams as shown in Fig. 3. This results in the two entangled beams having anticorrelated classical noise in the amplitude quadratures and correlated classical noise in the phase quadratures. Due to the 1:1 beam splitter ratio, both beams have an equal amount of added noise. The shares can then be expressed as

$$\hat{a}_1 = \frac{\hat{a}_\psi + \hat{a}_{\text{EPR}1} + \delta\hat{a}_{m1}}{\sqrt{2}} \quad (28)$$

$$\hat{a}_2 = \frac{\hat{a}_\psi - \hat{a}_{\text{EPR}1} - \delta\hat{a}_{m1}}{\sqrt{2}} \quad (29)$$

$$\hat{a}_3 = \hat{a}_{\text{EPR}2} + \delta\hat{a}_{m2} \quad (30)$$

where $\delta\hat{a}_{m1,2} = (\pm\delta\hat{X}_m^+ + i\delta\hat{X}_m^-)/2$ are the additional classical noise introduced by the two phase modulators. The strength of these additional modulations is given by $V_m^\pm = \langle(\delta\hat{X}_m^\pm)^2\rangle = e^{2s}$.

Similar to the previous dealer protocol, $\{1,2\}$ can retrieve the secret by completing a Mach-Zehnder interferometer. To reconstruct the secret, $\{2,3\}$ can interfere beams \hat{a}_2 and \hat{a}_3 on a 2/3 reflective beam splitter as shown in Fig. 3 [17]. The beams splitter outputs are given by

$$X_b^+ = \frac{1}{\sqrt{3}}(X_{\text{sqz}2}^- - X_{\text{sqz}1}^- + X_\psi^+ - 2X_m^+) \quad (31)$$

$$X_b^- = \frac{1}{\sqrt{3}}(X_{\text{sqz}1}^+ - X_{\text{sqz}2}^+ + X_\psi^-) \quad (32)$$

$$X_c^+ = \frac{[(X_{\text{sqz}1}^- - X_{\text{sqz}2}^-) - 3(X_{\text{sqz}1}^+ + X_{\text{sqz}2}^+) + 2(X_\psi^+ + X_m^+)]}{\sqrt{24}} \quad (33)$$

$$X_c^- = \frac{[(X_{\text{sqz}2}^+ - X_{\text{sqz}1}^+) - 3(X_{\text{sqz}1}^- + X_{\text{sqz}2}^-) + 2(X_\psi^- - 3X_m^-)]}{\sqrt{24}} \quad (34)$$

Since $X_{\text{sqz1,2}}^+ \ll 1$ in the limit of large squeezing. We note that the 2/3 reflective beam splitter ensures that the phase quadrature of the secret is already faithfully reconstructed in X_b^- . By measuring the amplitude fluctuations X_c^+ and applying them to X_b^+ , it is possible to eliminate the remaining anti-squeezed fluctuations, $X_{\text{sqz1,2}}^-$, and the classical amplitude noise X_m^+ on the same beam. This can be done simply by directly detecting beam \hat{c} and then electro-optically feeding the detected signal to the amplitude of beam \hat{b} with the right gain. Due to optical losses, however, better efficiency can be achieved by divorcing the modulators from beam \hat{b} as shown in Fig. 3. Instead the detected signal from beam \hat{c} is encoded off line on a strong local oscillator beam, a_{LO} . The signal on the local oscillator can then be mixed

back onto beam \hat{b} using a highly reflective beam splitter as shown in Fig. 3. The resulting output quadratures are given by $X_{\text{out}}^\pm = \sqrt{1-\epsilon}X_b^\pm + \sqrt{\epsilon}X_{\text{LO}}^\pm$. In the limit of high beam splitter reflectivity, $\epsilon \rightarrow 0$, we obtain

$$\begin{aligned} X_{\text{out}}^+ &\simeq X_b^+ + K(\omega)\delta I \\ X_{\text{out}}^- &\simeq X_b^- \end{aligned} \quad (35)$$

where $K(\omega)$ is a gain transfer function which takes into account the response of the electro-optic feedforward circuit and the loss due to the HR beam splitter. δI is the detected photocurrent of the amplitude quadrature fluctuations of beam \hat{c} given by

$$\delta I = \sqrt{\eta}\langle X_c^+ \rangle \left[\frac{1}{2}\sqrt{\frac{1}{3}}\sqrt{\eta} \left(\frac{1}{\sqrt{2}} (\delta X_{\text{sqz1}}^- - \delta X_{\text{sqz2}}^-) - \frac{3}{\sqrt{2}} (\delta X_{\text{sqz1}}^+ + \delta X_{\text{sqz2}}^+) + \sqrt{2} (\delta X_m^+ + \delta X_\psi^+) \right) + \sqrt{1-\eta}\delta X_d^+ \right] \quad (36)$$

where η and δX_d^+ are, respectively, the detection efficiency and the vacuum fluctuations due to an imperfect detector. The output quadrature fluctuations can be re-expressed as

$$\begin{aligned} \delta X_{\text{out}}^+ &= \left(\frac{1}{\sqrt{3}} + \frac{G}{\sqrt{6}} \right) \delta X_\psi^+ + \left(\frac{G}{2\sqrt{6}} - \frac{1}{\sqrt{3}} \right) (\delta X_{\text{sqz1}}^- - \delta X_{\text{sqz2}}^-) \\ &\quad - \frac{G}{2}\sqrt{\frac{3}{2}} (\delta X_{\text{sqz1}}^+ + \delta X_{\text{sqz2}}^+) + G\sqrt{\frac{1-\eta}{\eta}}\delta X_d^+ + \left(\frac{2}{\sqrt{3}} - \frac{G}{\sqrt{6}} \right) \delta X_m^+ \end{aligned} \quad (37)$$

$$\delta X_{\text{out}}^- = \sqrt{\frac{1}{3}}\delta X_\psi^- + \sqrt{\frac{1}{3}}(\delta X_{\text{sqz1}}^+ - \delta X_{\text{sqz2}}^+) \quad (38)$$

where $G = \eta K(\omega)\langle X_c^+ \rangle$ is the total gain of the feedforward loop. By setting $G = 2\sqrt{2}$, it is clear that the anti-squeezing and classical noise terms of Eq. (37) are cancelled. In the limit of perfect detection efficiency and large squeezing, we obtain

$$\delta X_{\text{out}}^+ = \sqrt{3}\delta X_\psi^+ \quad (39)$$

$$\delta X_{\text{out}}^- = \frac{1}{\sqrt{3}}\delta X_\psi^- \quad (40)$$

Hence {2,3} can reproduce a symplectically transformed version of the secret, \hat{a}_ψ . We note that since symplectic transformations are local unitary operation, no quantum information contained in the secret state is lost. Thus, the feedforward scheme works equally well when compared with the 2PSA scheme in terms of quantum information transfer. In order to reconstruct the quantum state of the secret, however, a single PSA is required on the output beam. Even so, the feedforward scheme is still technically less demanding than the 2PSA scheme introduced in the earlier section. In the next section, we will introduce experimental measures to characterize both QSS schemes.

V. CHARACTERIZATION

In teleportation experiments *fidelity*, $\mathcal{F} = \langle \psi_{\text{in}} | \rho_{\text{out}} | \psi_{\text{in}} \rangle$, is conventionally used to quantify the efficacy of a teleporter [14]. Fidelity can also be adopted to characterize QSS as it is a protocol that reconstructs input quantum states at a distance. If we assume that all input noise sources are Gaussian and that the secret is a coherent state, the fidelity of a QSS scheme is given by [15]

$$\mathcal{F} = 2e^{-(k^+ + k^-)} \sqrt{\frac{V_\psi^+ V_\psi^-}{(V_\psi^+ + V_{\text{out}}^+)(V_\psi^- + V_{\text{out}}^-)}} \quad (41)$$

where $k^\pm = \langle X_\psi^\pm \rangle^2 (1 - \langle X_\psi^\pm \rangle / \langle X_{\text{out}}^\pm \rangle)^2 / (4V_\psi^\pm + 4V_{\text{out}}^\pm)$. Assuming an ideal detector ($\eta = 1$), we obtain from the analysis of Section IV the theoretical limits of fidelity for the 2PSA scheme as a function of squeezing

$$\mathcal{F}_{\{1,2\}} = 1 \quad (42)$$

$$\mathcal{F}_{\{1,3\}} = \mathcal{F}_{\{2,3\}} = \frac{1}{1 + e^{-2r}} \quad (43)$$

where the subscripts i and j in $\mathcal{F}_{\{i,j\}}$ denote the collaborating players. We note that $\mathcal{F}_{\{1,2\}}$ is always unity since the re-

construction of secret only requires a simple Mach-Zehnder. In the limit of perfect entanglement, $r \rightarrow \infty$, the fidelity of Eq. (43) also approaches unity. In the case of the feedforward QSS scheme, however, we obtain

$$\mathcal{F}_{\{1,2\}} = 1 \quad (44)$$

$$\mathcal{F}_{\{1,3\}} = \mathcal{F}_{\{2,3\}} = e^{-\Gamma} \sqrt{\frac{3}{(2+e^{-2r})(2+3e^{-2r})}} \quad (45)$$

where Γ is dependent on the quadratures of the secret, $\langle X_{\psi}^{\pm} \rangle$, and the squeezing of the input states r , and is given by

$$\Gamma = \frac{2-\sqrt{3}}{12} \left[\langle X_{\psi}^+ \rangle^2 \frac{1}{(2+3e^{-2r})} + \langle X_{\psi}^- \rangle^2 \frac{9}{(2+e^{-2r})} \right] \quad (46)$$

Equation (45) does not tend to unity even in the limit of infinite input squeezing. In fact, it quickly degrades to zero for finite squeezing and large secret sideband modulations. The reason for this is due to the symplectically transformed secret output state \hat{a}_{out} . We point out, however, that no information is lost. Indeed $\{2,3\}$ can locally transform the output to get back the original secret state via a single parametric process. The fidelity given in Eq. (45) after the parametric correction then becomes equal to that of Eq. (43).

An alternative measure that is invariant to symplectic transformations is the T-V graph proposed by Ralph and Lam [16], and used to characterize quantum teleportation [15]. This

graph plots the product of the conditional variances of both conjugate observables $V_q = V_{cv}^+ V_{cv}^-$ against the sum of the signal transfer coefficients $T_q = T^+ + T^-$. Here the conditional variances are given by

$$V_{cv}^{\pm} = V_{\text{out}}^{\pm} + \frac{|\langle \delta X_{\psi}^{\pm} \delta X_{\text{out}}^{\pm} \rangle|}{V_{\psi}^{\pm}} \quad (47)$$

and the signal transfer coefficients are defined as

$$T^{\pm} = \frac{SNR_{\text{out}}^{\pm}}{SNR_{\psi}^{\pm}} \quad (48)$$

In contrast to fidelity which measures the quality of the state reconstruction, the T-V graph emphasizes the transfer of quantum information [15]. In an ideal QSS scheme, collaborating players would obtain $T_q = 2$ and $V_q = 0$.

Using these measures, the collaborating players using the 2PSA scheme can obtain

$$T_q = \frac{2}{1+2e^{-2r}} \quad (49)$$

$$V_q = 2e^{-2r} \quad (50)$$

Whilst for the feedforward scheme the collaborating players, which we will now denote as (CP), can obtain

$$T_q^{\text{CP}} = \frac{1}{1+2e^{-2r}} + \frac{(1 + \frac{G}{\sqrt{2}})^2}{\left(1 + \frac{G}{\sqrt{2}}\right)^2 + \left(\frac{G}{2} - \sqrt{2}\right)^2 e^{2r} + \left(\frac{3G}{2}\right)^2 e^{-2r} + \left(2 - \frac{G}{\sqrt{2}}\right)^2 e^{2s} + \frac{3G^2(1-\eta)}{\eta}} \quad (51)$$

$$V_q^{\text{CP}} = \frac{e^{-2r}}{18} \left[9G^2 e^{-2r} + e^{2r} (G - 2\sqrt{2})^2 + 2e^{2s} (G - 2\sqrt{2})^2 + 12G^2 \left(\frac{1-\eta}{\eta}\right) \right] \quad (52)$$

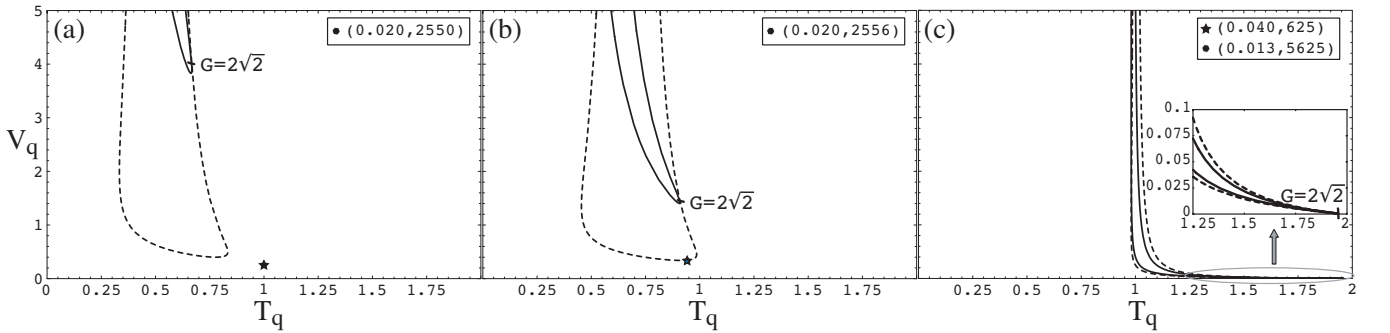


FIG. 4: T-V graphs for the feedforward scheme with (a) no squeezing, (b) 40% of squeezing, and (c) 99% of squeezing. The lines represent the information retrieved by $\{2,3\}$ with varying feedforward gain, and the points represent the information retrieved by $\{1\}$ or $\{2\}$ alone. The dashed lines and stars correspond to the absence of added modulations, whilst the solid lines and circles correspond to 20dB above the quantum noise of added modulations. We have assumed perfect detector efficiency for the feedforward loop. The coordinates of the points which are not outside of the plotted region are displayed in the inset of each graph.

where e^{2s} is the power of the added classical noise. Before

analysing these results, we first determine the amount of in-

formation the single players (SP), i.e. the adversary structures, can learn about the secret if they were to measure their shares directly. In this situation, T_q^{SP} and V_q^{SP} for the single players are found to be

$$T_q^{\text{SP}} = \frac{2}{1 + \cosh 2r + e^{2s}} \quad (53)$$

$$V_q^{\text{SP}} = \frac{(\cosh 2r + e^{2s})^2}{4} \quad (54)$$

Figure 4 shows the results of the feedforward QSS scheme for three different amounts of input squeezing. The dotted lines represent the results obtained by $\{2,3\}$ in the absence of added classical noise when feedforward gain is varied. The star points represent the maximum information retrievable by $\{1\}$ or $\{2\}$ alone in the corresponding situations. Results for the addition of classical noise, 20 dB above the quantum noise limit, are depicted by solid lines for the collaborating players and by circles for the single players. In the limit of infinite input squeezing, the collaborating players can reconstruct the secret perfectly, with $T_q^{\text{CP}} \rightarrow 2$ and $V_q^{\text{CP}} \rightarrow 0$. This is achieved with an optimum, feedforward gain of $G = 2\sqrt{2}$ where the influence of both the anti-squeezing quadratures (and the added classical noise) are completely cancelled as discussed in Section IV B. Whilst single players in the same limit obtain no information about the secret, with $T_q^{\text{SP}} \rightarrow 0$ and $V_q^{\text{SP}} \rightarrow \infty$, due to the dominant effect of the anti-squeezing quadratures (and the added classical noise). These results are shown in the plots of Fig. 4(c). In the case of finite squeezing and no added classical noise, however, the optimum feedforward gain for the collaborating players is always less than $2\sqrt{2}$ as shown in both Fig. 4(a) and (b). Further, single players forming the adversary structures can obtain some quantum information about the secret. When the amount of input squeezing less than 42%, single players obtain more quantum information than the access structures using the feedforward protocol. In this situation, the collaborating players should directly measure their shares containing the secret. The classical limit obtained when there is no input squeezing and no added classical noise is then $T_q^{\text{SP}} = T_q^{\text{CP}} = 1$ and $V_q^{\text{SP}} = V_q^{\text{CP}} = 1/4$, as shown by the star point of Fig. 4(a).

In order to prevent the single players from obtaining information about the secret, the dealer can introduce phase quadrature noise on both input amplitude squeezed beams. The phase noise translates to added noise in both the amplitude and phase quadratures of the entangled beams, δX_m^\pm . For large modulations, say 20 dB above the quantum noise limit, the single players obtain virtually no information about the secret, thus making $T_q^{\text{SP}} \rightarrow 0$ and $V_q^{\text{SP}} \rightarrow \infty$ even in the absence of input squeezing. Collaborating players on the other hand, obtain a zero squeezing classical limit of $T_q^{\text{CP}} \rightarrow 2/3$

and $V_q^{\text{CP}} \rightarrow 4$.

Another consequence of the added classical noise for the collaborating players is that the optimum gain for maximum information transfer again approaches $2\sqrt{2}$. This results in the collaborating players obtaining less information about the secret with increasing classical noise. Nonetheless, the collaborating players can now obtain much more information than the single players for all levels of input squeezing. Any amount of input squeezing will now differentially increase the amount of information the access structure has over the adversary structure. These results are illustrated by the solid lines and the circles of Fig. 4.

VI. CONCLUSION

(T_q, V_q)		clas, \bar{n}	clas,n	quan, \bar{n}	quan,n
Adversary	1	(1,1/4)	(0, ∞)	(0, ∞)	(0, ∞)
Structure	2	(1,1/4)	(0, ∞)	(0, ∞)	(0, ∞)
	3	(0,1)	(0, ∞)	(0, ∞)	(0, ∞)
Access	$\{1,2\}$	(2,0)	(2,0)	(2,0)	(2,0)
Structure	$\{1,3\}$	(1,1/4)	(2/3,4)	(2,0)	(2,0)
	$\{2,3\}$	(1,1/4)	(2/3,4)	(2,0)	(2,0)

TABLE I: Summary of the performances of the feedforward QSS schemes with (quan) and without (clas) optical entanglement; and with (n) and without added noise (\bar{n}). Parameters listed are the best achievable (T_q, V_q) values.

In this paper, we presented two experimental (2,3) threshold QSS schemes. The first one requires a pair of optically entangled beams and two phase sensitive amplifiers for the reconstruction of the secret state. Whilst the second utilizes a pair of optically entangled beams and an additional electro-optic feedforward loop. We have shown that although the latter does not exactly reproduce the original secret state, all quantum information is retained in the reconstructed output state in the limit of perfect entanglement. We show that by introducing controlled classical modulations on the entangled beams, it is possible to insure security against attacks from individual players. Table I summarizes the performances of our proposed feedforward QSS scheme for both classical (without entanglement), and quantum (with perfect entanglement) regimes. They are also calculated for situations with and without added classical noise.

This research is supported by the Australian Research Council. We thank Ben Buchler and Stephen Bartlett for useful discussions. This work is a part of EU QIPC Project, No. IST-1999-13071 (QUICOV).

[1] M. Hillery et al, Phys. Rev. A **59**, 1829 (1999).
[2] A. Shamir, Comm. of the ACM **22**, 612 (1979).
[3] R. Cleve et al, Phys. Rev. Lett. **83**, 648 (1999).
[4] T. Tyc, and B. C. Sanders, Phys. Rev. A **65**, 42310 (2002).

[5] L. Vaidman, Phys. Rev. A **49**, 1473 (1994); S. L. Braunstein and H. J. Kimble, Phys. Rev. Lett. **80**, 869 (1998); A. Furusawa et al, Science **282**, 706 (1998).
[6] J. A. Levenson, I. Abram, T. Rivera and P. Grangier, JOSAB

- 10**, 2233 (1993).
- [7] P. K. Lam, T. C. Ralph, B. C. Buchler, D. E. McClelland, H-A. Bachor, and J. Gao., *J. Opt. B* **1**, 469 (1999).
- [8] M. Reid, *Phys. Rev. A* **40**, 913 (1989).
- [9] K. Bencheikh, T. Symul, A. Jankovic, and J. A. Levenson, *J. of Mod. Opt.* **48**, 1903 (2001).
- [10] Z. Y. Ou, S. F. Pereira, H. J. Kimble, and K. C. Peng, *Phys. Rev. Lett.* **68**, 3663 (1992).
- [11] L-M. Duan *et al.*, *Phys. Rev. Lett.* **84**, 2722 (2000).
- [12] P. K. Lam, T. C. Ralph, E. H. Huntington and H-A. Bachor, *Phys. Rev. Lett.* **79**, 1471 (1997); T. C. Ralph, *Phys. Rev. A* **56**, 4187 (1997); E. H. Huntington, P. K. Lam, T. C. Ralph, D. E. McClelland and H-A. Bachor, *Opt. Lett.* **23**, 540 (1998).
- [13] B. C. Buchler, P. K. Lam, and T. C. Ralph, *Phys. Rev. A* **60**, 4943 (1999).
- [14] A. Furusawa *et al.*, *Science* **282**, 706 (1998).
- [15] W. P. Bowen, N. Treps, B. C. Buchler, R. Schnabel, T. C. Ralph, H-A. Bachor, T. Symul and P. K. Lam, [quant-ph/0207179](https://arxiv.org/abs/quant-ph/0207179).
- [16] T. C. Ralph, P. K. Lam and R. E. S. Polkinghorne, *J. Opt. B* **1**, 483 (1999).
- [17] In this paper, a 2:1 beam splitter ratio is adopted for the analysis of the secret reconstruction between $\{2,3\}$ for all situations. We note that in general, both the beam splitter ratio and the feedforward gain can be optimised depending on the amount of input entanglement.